Spectrochimica Acta Part A 78 (2011) 1180–1186

Contents lists available at ScienceDirect

Spectrochimica Acta Part A: Molecular and Biomolecular Spectroscopy

journal homepage: www.elsevier.com/locate/saa

Absorption spectroscopic probe to investigate the interaction between Nd(III) and calf-thymus DNA

Ch. Victory Devi, N. Rajmuhon Singh*

Department of Chemistry, Manipur University, Canchipur, Imphal 795 003, Manipur, India

ARTICLE INFO

Article history:
Received 27 September 2010
Received in revised form
15 December 2010
Accepted 25 December 2010

Keywords:
Nd(III)
4f–4f transition spectra
Calf-thymus DNA
Oscillator strength
Judd–Ofelt parameters

ABSTRACT

The interaction between Nd(III) and Calf Thymus DNA (CT-DNA) in physiological buffer (pH 7.4) has been studied using absorption spectroscopy involving 4f–4f transition spectra in different aquated organic solvents. Complexation with CT-DNA is indicated by the changes in absorption intensity following the subsequent changes in the oscillator strengths of different 4f–4f bands and Judd–Ofelt intensity (T_λ) parameters. The other spectral parameters namely Slator–Condon (F_k's), nephelauxetic effect (β), bonding ($b^{1/2}$) and percent covalency (δ) parameters are computed to correlate with the binding of Nd(III) with DNA. The absorption spectra of Nd(III) exhibited hyperchromism and red shift in the presence of DNA. The binding constant, K_b has been determined by absorption measurement. The relative viscosity of DNA decreased with the addition of Nd(III). Thermodynamic parameters have been calculated according to relevant absorption data and Van't Hoff equation. The characterisation of bonding mode has been studied in detail. The results suggested that the major interaction mode between Nd(III) and DNA was external electrostatic binding.

1. Introduction

Nucleic acids play an important role in biological systems and carry out a broad range of biological functions. Increasing interest is being shown in DNA because of their application in various type of therapy [1]. The biological function of DNA is often dependent on interactions with different moieties such as metal ions [2,3]. DNA structure can undergo conformational changes due to ligand binding. Metal ions are important cofactors in DNA structures and function, facilitating the double helical structure stabilization and catalysis [4]. Also the extent of hydration of cations bound to DNA is a key parameter in the energies of the binding process as well as a relevant issue in the catalytic roles and structural effects of bound ions. An understanding of the factors involved in metal ion–DNA interaction is thus of considerable importance.

Trivalent lanthanide ions form a relatively homogeneous group of 15 elements having attractive, spectroscopic and magnetic properties [5], and have been used as probes of the interactions of metal ions with nucleic acids [6] and other polyelectrolyte [7]. Nucleic acid may be considered to be ambidentate ligands, with various potential binding sites, including nitrogen and oxygen donor on the bases, hydroxyl groups on the ribose sugar, and negatively charged oxygen atoms in the phosphate groups. As a consequence of the abundant of negatively charged oxygen donor groups, the DNA molecule readily interact with Ln^{3+} ions and may be expected to occupy at least some of the inner sphere coordination sites of the cations, contributing to the coordination process by completing chelate-bridges [8]. Nd(III) possess many similarities in their properties to Ca(II) and isomorphous replacement of this cation by Ln^{3+} ions holds out the promise of exploiting the rich and variety of spectroscopic properties of the lanthanides for obtaining information in their application to biomolecular structure examination [9,10]. In last few years, time-resolved capability of lanthanide luminescent bioprobes (LLBS) [11] and the availability of adequate bioconjugation protocols [12] allowed the development of highly sensitive immunoassays [13,14], protein staining assays [15], nucleic acid analysis [16], or the determination of enzyme activities [17]. This bio-application has been a major factor in the unprecedented expansion of lanthanide coordination chemistry during the past 20 years. In addition, the absorption spectra of the trivalent lanthanides have been of interest to both chemists and spectroscopists. Misra [18] had studied about the interaction of Pr(III) with nucleosides and nucleotides in different stoichiometries in water and water–DMF mixture by employing absorption difference and comparative spectrophotometry. These studies indicated that the binding of the nucleotide is through phosphate oxygen in a bidentate manner and the complexes undergo substantial ionisation in aqueous medium. Joseph et al. [19] had reported about the absorption spectral studies on the interaction of adenine, adenosine 5′-mono, adenosine-5′-di and adenosine 5′-triphosphate with Pr(III) in different stoichiometries and at varying hydrogen ion concentration.

* Corresponding author. Tel.: +91 9436080780; fax: +91 3852435145.
E-mail address: rajmuhon@yahoo.co.in (N.R. Singh).

1386-1425/$ – see front matter © 2010 Elsevier B.V. All rights reserved.
doi:10.1016/j.saa.2010.12.078

The main aim of our study is to find the mode of the interaction between Nd(III) with Calf-Thymus DNA using absorption difference and comparative absorption spectroscopy involving 4f–4f transitions and viscosity measurement. Thermodynamic parameters have been calculated according to relevant absorption data and Van't Hoff equation. The interaction mechanism and binding mode is studied in detail. The sensitivity of 4f–4f bands towards the minor coordination environment around the metal ion is also used in selected different aquated organic solvents and the corresponding changes in oscillator strengths of different 4f–4f bands and experimentally determined Judd–Ofelt intensity (T_λ) parameters are correlated with the binding of DNA.

2. Experimental

2.1. Materials

Neodymium nitrate hexahydrate of 99.9% purity is purchased from CDH, Mumbai and Calf Thymus DNA from Sigma is used as supplied. The solvents used are MeCN, MeOH, DMF and Dioxane of AR. Grade from E Merk.

All the experiments involving interaction of the Nd(III) with Calf-Thymus DNA are formed in Tris–HCl (0.01 M, pH 7.4). Solutions of CT-DNA in buffer gave a ratio of UV absorbance at 260 and 280 nm, A_{260}/A_{280}, of 1.8–1.9 indicating that DNA is free from protein [20]. The DNA concentration is measured by its absorbance at 260 nm using the molar extinction coefficient 6600 M^{-1} cm^{-1}. Double distilled water was used to prepare all stock solutions for DNA binding studies. The absorption spectral data are recorded on Perkin Elmer Lambda-35 UV-Vis Spectrometer equipped with a device for kinetic and high resolution spectral analysis. The temperature of all observations is maintained using Perkin Elmer PTP1 Peltier-temperature system at 25 °C.

Viscosity measurements are conducted on a Rheometer (BRUKER), immersed in a thermostated water bath maintained at 25 °C. Titrations are performed by the addition of aliquots of the Nd(III) (1×10^{-4}–5×10^{-4} mM) solution into a constant concentration of DNA in the viscometer. Data are presented as $(\eta/\eta_0)^{1/3}$ versus the concentration of Nd(III), η is the viscosity of DNA in the presence of Nd(III) and η_0 is the viscosity of DNA alone.

2.2. Methods

The energy of 4f–4f transitions comprises of two main components: coulombic F_k and spin–orbit coupling 4f parameters, represented in the form of equation as follows

$$E_{\text{obs}} = f^k F_k + A_{\text{so}}\xi_{4f} \tag{1}$$

where f^k and A_{so} are the angular counterpart of coulombic and spin-orbit interaction, while F_k (Slator–Condon inter-electronic parameter) and ξ_{4f} are the radial integral known as Lande's parameter. The values of inter-electronic repulsion parameters i.e. Slator–Condon, F_k's and spin–orbit coupling Lende's parameter, ξ_{4f} are determined using the method outlined in our earlier papers [21,22].

If the f-orbital's are involved in covalent bond formation with the ligand, the metal wave function can be expressed [23] as

$$\langle\varphi_{4f} = (1-b)^{1/2}\langle 4f| - b^{1/2}\langle\varphi_{\text{ligand}}| \tag{2}$$

where $b^{1/2}$ measures the amount of 4f-orbital mixing, i.e. covalency. Sinha [24] has proposed a δ scale to express the covalency. Both the parameters $b^{1/2}$ and δ are related to the nephelauxetic effect, i.e. β. The covalency parameter (β, $b^{1/2}$, δ) of the complexes have been calculated using the relationship [23–25]:

$$\beta = \frac{F_k^c}{F_k^f} \quad \text{or} \quad \beta = \frac{E_c^k}{E_f^k} \tag{3}$$

where F_k^c (k = 2,4,6) and E_c^k are the Slator–Condon and Racah parameters for complex, and F_k^f and E_f^k for free ions respectively.

$$b^{1/2} = \left[\frac{1-\beta}{2}\right]^{1/2} \tag{4}$$

$$\delta = \left(\frac{1-\beta}{\beta}\right) \times 100 \tag{5}$$

The intensity of the absorption band is measured by experimentally determined oscillator strength (P_{obs}), which is directly proportional to the area under the absorption curve and is found out by Gaussian curve analysis [26] as

$$P = 4.6 \times 10^{-9} \times \varepsilon_{\max} \times \Delta\upsilon_{1/2} \tag{6}$$

where $\varepsilon_{\max}$ is the molar extinction coefficient and $\Delta\upsilon_{1/2}$ is the half band width. The calculated oscillator strength of the induced dipole transition $\pi J \rightarrow \pi' J'$ of the energy (cm^{-1}) in accordance with Judd [27] and Ofelt [28] can be expressed as

$$P_{\text{cal}} = \sum_{k=2,4,6} T_\lambda \upsilon \left\langle f^n \psi_J || U^{(\lambda)} || f^n \psi_{J'} \right\rangle^2 \tag{7}$$

which can be reduced to

$$\frac{P_{\text{cal}}}{\upsilon} = \left[U^{(2)}\right]^2 \cdot T_2 + \left[U^{(4)}\right]^2 \cdot T_4 + \left[U^{(6)}\right]^2 \cdot T_6 \tag{8}$$

where $U^{(\lambda)}$ is the matrix element of unit tensor operator connecting initial $\langle f^n \psi_j|$ and final $|f^n \psi_{j'}\rangle$ through three phenomenological parameters T_λ (λ = 2,4,6) called Judd–Ofelt parameters. These parameters are related to the radial wave function of the states and ligand field parameters that characterise the surrounding field. The three parameters T_2, T_4 and T_6 are related to the radial part of the $4f^n$ wavefunction of the perturbing configuration. The values of T_λ parameters have been computed using the matrix elements given in our earlier paper [29].

3. Results and discussion

Since lanthanides are hard metal ions and thus, their preference will be for hard donor sites like the oxygen atom and hence their bonding is basically electrostatic in nature. The interaction of CT-DNA to Nd(III) should bring about the lowering of energy interaction parameters. However, data in Table 1 and Table 2 shows only slight variation as compared to the values for free ion taken as standard. The positive value of $b^{1/2}$ indicates the incidence of some covalent character in the metal–ligand bonding leading to nephelauxetic effect. Therefore, the changes in the energy interaction parameters are not apparently significant. We gave more emphasis to quantitative f–f transition intensity analysis because changes in intensities are more significant compared to energy. The absolute values of oscillator strengths and Judd–Ofelf intensity (T_λ) intensity parameters are determined under different experimental conditions for Nd(III) complexes with CT-DNA (Table 3). This clearly suggests a significant enhancement in the oscillator strengths of different 4f–4f transitions. As a consequence, we have observed noticeable increase in the magnitude of Judd–Ofelt (T_λ) intensity parameters. These suggests the binding of the CT-DNA to Nd(III) in solution.

The effect of solvent on complexation is quite significant. Comparative absorption spectra of Nd(III):CT-DNA in different aquated organic solvents (Fig. 1) clearly suggest the affinity of solvents

Table 1
Computed values of energy interaction F_k (cm^{-1}), nephelauxetic effect (β), bonding ($b^{1/2}$) and covalency (δ) parameters for Nd(III) and Nd(III):CT-DNA (1:1) at 298 K in different aquated organic solvents.

System	F_2	F_4	F_6	β	$b^{1/2}$	δ
Water						
Nd(III)	332.03	48.65	5.10	0.9926	0.061	0.7472
Nd(III):CT-DNA	332.03	48.65	5.10	0.9927	0.060	0.7345
MeCN	331.98	48.63	5.10	0.9932	0.058	0.6796
Nd(III)	331.99	48.64	5.11	0.9934	0.057	0.6671
Nd(III):CT-DNA	331.98	48.63	5.11	0.9932	0.058	0.6796
DMF						
Nd(III)	332.11	48.68	5.10	0.9925	0.061	0.7546
Nd(III):CT-DNA	332.10	48.67	5.10	0.9925	0.061	0.7544
Dioxane						
Nd(III)	332.02	48.67	5.11	0.9931	0.058	0.6908
Nd(III):CT-DNA	332.00	48.67	5.11	0.9931	0.058	0.6956
MeOH						
Nd(III)	332.00	48.64	5.10	0.9930	0.059	0.704
Nd(III):CT-DNA	332.00	48.64	5.10	0.9930	0.059	0.704
MeCN:Dioxane(1:1)						
Nd(III)	332.02	48.66	5.11	0.9932	0.058	0.6685
Nd(III):CT-DNA	332.01	48.63	5.11	0.9934	0.057	0.6646
DMF:Dioxane (1:1)						
Nd(III)	331.91	48.63	5.11	0.9940	0.054	0.6053
Nd(III):CT-DNA	331.90	48.62	5.11	0.9940	0.054	0.6006
DMF:MeCN (1:1)						
Nd(III)	331.91	48.63	5.11	0.9940	0.055	0.6042
Nd(III):CT-DNA	331.91	48.64	5.11	0.9939	0.055	0.6123
MeCN:Dioxane(1:1)						
Nd(III)	332.02	48.64	5.11	0.9932	0.058	0.6874
Nd(III):CT-DNA	332.03	48.65	5.10	0.9929	0.059	0.7170
MeOH:MeCN(1:1)						
Nd(III)	332.00	48.65	5.11	0.9932	0.058	0.6883
Nd(III):CT-DNA	332.01	48.65	5.11	0.9931	0.058	0.6933
MeOH:DMF(1:1)						
Nd(III)	331.90	48.63	5.11	0.9941	0.054	0.5909
Nd(III):CT-DNA	331.92	48.64	5.12	0.9943	0.053	0.5768

towards the Nd(III) coordination. DMF appears to have strongest complexation influence on Nd(III):CT-DNA complexes followed by Dioxane and least in acetonitrile. This means that DMF has larger impact in promoting 4f–4f electric dipole intensity, which is in accordance with our previous studies [30]. The difference in oscillator strength in different solvents may be associated to ligand (solvent) structure and their coordination behaviours. The DMF has two coordination sites but it generally binds via oxygen when it coordinates to hard acids like lanthanides. The red shift is observed in the energies of all the five bands which are considered as marker for quantitative analysis in Nd(III) ion i.e. $^4I_{9/2} \rightarrow {}^4G_{5/2}$ ($^4I_{9/2}$ is ground state for Nd(III) ion and $^4G_{7/2}$, $^4F_{7/2}$, $^4F_{5/2}$, $^4F_{3/2}$ are internal excited state for pNd(III) ion) the hypersensitive transition and other transitions, $^4I_{9/2} \rightarrow {}^4G_{7/2}$, $^4I_{9/2} \rightarrow {}^4F_{3/2}$, $^4I_{/2} \rightarrow {}^4F_{5/2}$, and $^4I_{9/2} \rightarrow {}^4F_{7/2}$. These transitions, other than hypersensitive, do not obey $|J|$ selection rules and hence can only be considered as pseudo-hypersensitive [31]. The relative sensitivity of all the five transitions can be best explained through the plot of oscillator strengths as a function of T_2^c/T_2^a ("c" for complex ion and "a" for aquo ion). This shows the following order of relative sensitivity for all the five bands of Nd(III) ion; $^4G_{5/2} > {}^4G_{7/2} > {}^4F_{7/2} > {}^4F_{5/2} > {}^4F_{3/2}$ as highest value of slope is found for hypersensitive transition i.e. $^4G_{5/2}$ and lowest value for pseudo-hypersensitive transition, $^4F_{3/2}$.

Although we have found red shift in energies of all transitions, the effect is found pronounced in DMF. The red shift is due to the expansion of the metal orbital radius which leads to nephelauxetic effect. At the same time, the nephelauxetic effect brings about a shortening of the metal–ligand bond length thereby increasing the probability of interaction between metal and ligand orbital. Jorgensen and Ryan [32] noticed the dependence of the nephelauxetic effect on the coordination number and suggested the shortening in the metal–ligand distance occurs with the decrease in the coordination number. To interpret the correlation, analy-

Table 2
Observed and calculated values of energy (cm^{-1}) for Nd(III) and Nd(III):CT-DNA (1:1) at 298 K in different aquated organic solvents.

System	$^4F_{3/2}$, E_{obs} (E_{cal})	$^4F_{5/2}$, E_{obs} (E_{cal})	$^4F_{7/2}$, E_{obs} (E_{cal})	$^4G_{5/2}$, E_{obs} (E_{cal})	$^4G_{7/2}$, E_{obs} (E_{cal})
Water					
Nd(III)	11,558 (11,551)	12,590 (12,626)	13,510 (13,466)	17,409 (17,390)	19,172 (19,174)
Nd(III):CT-DNA	11,558 (11,552)	12,591 (12,627)	13,510 (13,466)	17,410 (17,390)	19,173 (19,175)
MeCN					
Nd(III)	11,550 (11,550)	12,590 (12,612)	13,510 (13,466)	17,386 (17,405)	19,172 (19,175)
Nd(III):CT-DNA	11,557 (11,550)	12,590 (12,626)	13,510 (13,466)	17,387 (17,405)	19,170 (19,174)
DMF					
Nd(III)	11,559 (11,554)	12,591 (12,627)	13,511 (13,466)	17,387 (17,412)	19,117 (19,179)
Nd(III):CT-DNA	11,560 (11,554)	12,591 (12,627)	13,511 (13,466)	17,387 (17,412)	19,178 (19,176)
Dioxane					
Nd(III)	11,556 (11,551)	12,590 (12,626)	13,509 (13,466)	17,387 (17,407)	19,175 (19,176)
Nd(III):CT-DNA	11,557 (11,551)	12,591 (12,626)	13,508 (13,466)	17,388 (17,407)	19,174 (19,175)
MeOH					
Nd(III)	11,559 (11,551)	12,590 (12,626)	13,509 (13,466)	17,387 (17,407)	19,175 (19,176)
Nd(III):CT-DNA	11,559 (11,551)	12,590 (12,626)	13,510 (13,466)	17,387 (17,407)	19,171 (19,174)
MeCN:Dioxane (1:1)					
Nd(III)	11,555 (11,551)	12,591 (12,626)	13,510 (13,466)	17,388 (17,407)	19,175 (19,175)
Nd(III):CT-DNA	11,555 (11,550)	12,591 (12,626)	13,511 (13,466)	17,385 (17,405)	19,172 (19,174)
DMF:Dioxane (1:1)					
Nd(III)	11,556 (11,547)	12,588 (12,624)	13,509 (13,466)	17,383 (17,400)	19,168 (19,174)
Nd(III):CT-DNA	11,556 (11,547)	12,589 (12,624)	13,509 (13,466)	17,383 (17,399)	19,166 (19,174)
DMF:MeCN (1:1)					
Nd(III)	11,556 (11,547)	12,588 (12,624)	13,509 (13,466)	17,383 (17,400)	19,167 (19,174)
Nd(III):CT-DNA	11,555 (11,547)	12,588 (12,624)	13,509 (13,465)	17,384(17,400)	19,168 (19,174)
MeOH:Dioxane (1:1)					
Nd(III)	11,560 (11,551)	12,591 (12,626)	13,510 (13,466)	17,382 (17,407)	19,173 (19,175)
Nd(III):CT-DNA	11,559 (11,552)	12,591 (12,626)	13,510 (13,466)	17,386 (17,408)	19,173 (19,175)
MeOH:MeCN (1:1)					
Nd(III)	11,556 (11,551)	12,588 (12,624)	13,509 (13,466)	17,382 (17,399)	19,167 (19,174)
Nd(III):CT-DNA	11,557 (11,551)	12,590 (12,626)	13,510 (13,466)	17,387 (17,407)	19,173 (19,175)
MeOH:DMF (1:1)					
Nd(III)	11,555 (11,546)	12,588 (12,624)	13,509 (13,4660)	17,382 (17,399)	19,167 (19,174)
Nd(III):CT-DNA	11,554 (11,546)	12,588 (12,624)	13,509 (13,465)	17,381 (17,398)	19,169 (19,175)

Table 3
Observed oscillator strength ($P \times 10^6$) and Judd–Ofelt ($T \times 10^{10}$) parameters for Nd(III) and Nd(III)–CT-DNA (1:1) at 298 K in different aquated organic solvents.

System	$^4F_{3/2}$	$^4F_{5/2}$	$^4F_{7/2}$	$^4G_{5/2}$	$^4G_{7/2}$	T_2	T_4	T_6
Water								
Nd(III)	0.265	1.557	1.959	1.531	0.401	7.86	1.25	34.13
Nd(III):CT-DNA	0.276	1.661	2.097	1.759	0.540	9.90	0.02	35.08
MeCN								
Nd(III)	0.269	1.614	2.049	2.255	0.593	14.63	0.85	34.80
Nd(III):CT-DNA	0.264	1.682	2.202	2.313	0.843	26.28	0.96	39.49
DMF								
Nd(III)	0.342	1.588	2.012	2.086	0.553	11.25	1.81	33.02
Nd(III):CT-DNA	0.346	2.679	2.213	2.356	0.617	13.35	0.77	36.13
Dioxane								
Nd(III)	0.072	1.706	1.856	1.944	0.330	8.27	2.50	33.86
Nd(III):CT-DNA	0.367	1.564	1.885	1.735	0.364	8.74	2.41	31.33
MeOH								
Nd(III)	0.282	1.535	2.054	2.243	0.419	13.73	1.56	34.01
Nd(III):CT-DNA	0.283	1.637	2.012	2.185	0.378	13.84	1.47	34.13
MeCN:Dioxane (1:1)								
Nd(III)	0.199	1.312	1.720	2.695	0.597	12.44	0.51	28.51
Nd(III):CT-DNA	0.125	1.482	1.861	1.939	0.367	13.03	4.08	32.12
DMF:Dioxane (1:1)								
Nd(III)	2.465	1.365	1.673	2.001	0.189	10.07	0.14	34.03
Nd(III):CT-DNA	2.495	1.396	1.891	2.054	0.226	10.32	9.23	14.85
DMF:MeCN (1:1)								
Nd(III)	0.289	1.764	2.259	2.039	0.577	11.83	0.491	37.74
Nd(III):CT-DNA	0.269	1.756	2.429	2.272	0.615	14.30	2.79	40.07
MeOH:Dioxane (1:1)								
Nd(III)	0.357	1.284	1.604	2.490	0.378	13.69	2.68	26.03
Nd(III):CT-DNA	0.254	1.17	1.57	1.78	0.24	10.80	0.97	25.99
MeOH:MeCN (1:1)								
Nd(III)	0.312	1.771	2.161	2.004	0.509	11.21	2.64	39.35
Nd(III):CT-DNA	0.325	1.791	2.161	2.042	0.601	10.88	1.83	36.34
MeOH:DMF (1:1)								
Nd(III)	0.292	1.459	1.773	2.381	0.362	14.60	1.41	32.50
Nd(III):CT-DNA	0.280	1.481	1.852	2.481	0.384	15.08	0.89	30.60

sis of the relationship between nephelauxetic effect, geometry and energy parameters have been derived and evaluated for complex compounds using the angular overlap model, the value of "n" is proportional to the nephelauxetic effect,

$$n = \left[\frac{(1-\beta^{1/2})}{\beta^{1/2}}\right] \tag{9}$$

It may be expressed as

$$n = \left\{\frac{H^2 L}{(H_M - H_L)^2}\right\}(S*R)^2 N \tag{10}$$

where N is the coordination number, H_M and H_L are coulomb integrals of the atomic orbital, S is the overlap integral, R is the radius of the orbit. For compounds with ligands coordinated through identical donor atoms, the 1st terms of the RHS of Eq. (10) is a constant and Eq. (10) then becomes

$$n = \text{constant}\,(S*R)^2 N \tag{11}$$

Eq. (11) represents the nephelauxetic effect as a function of two variables, S^*R and N, which vary with changes in lanthanide–ligand distance in opposite directions. However, any variation in the values of R leads to a larger change in $(S^*R)^2$ compared to that in N. As a result, the nephelauxetic effect increases when the coordination number decreases. The Ln–O distance shortens in spite of the additive nature of β and decrease in the number of co-ordinating ligands. Frey and Horrocks [33] confined this study on Eu^{3+} and suggested that the nephelauxetic effect is related with the covalency in the metal–ligand bond and with the coordination number (lower the coordination number higher is the magnitude of nephelauxetic effect). The analysis of the oscillator strengths and Judd–Ofelt (T_λ) intensity parameters are used in the investigation of formation and nature of Nd(III)-DNA complexes. The high values of the T_2 parameter are remarkable indicating very intense hypersensitive transitions compared with the same transitions in aqueous solution. The intensity enhancement can be attributed to the high polarisability of DNA and to the anisotropy of this polarisability. According to the ligand polarisation model [34–36], the radiation field of the light dynamically polarises the ligand charge distributions and the instantaneous dipoles couple to the induced electric dipoles of the lanthanide ion. The low site symmetry of the complex promotes intense f–f transitions, because in an asymmetric environment it is more unlikely that some of the odd crystal field parameter (necessary for mixing states of opposite parity in to the 4f states) will have a very small value or will vanish [34]. Additionally part of the intensity enhancement of the hypersensitive transition can be attributed to the replacement of water by DMF as solvent [37]. The values of T_4 and T_6 parameters of the complexes are not significantly larger than the corresponding values in aqueous solution. The insensitivity of T_4 and T_6 in comparison with T_2 can be explained by the ligand polarisation distribution to these parameters are small.

Table 3 clearly reflect, that T_4 and T_6 are effected significantly in the presence of different solvents, suggest that not only immediate coordination environment of Nd(III) but symmetry of the complex species is also changed dramatically. These changes are considered to be good evidence for the involvement of DNA in the inner sphere coordination of Nd(III) ion. Though the ligand environment has only weak influence on the electronic cloud of the Nd(III), the 4f shell is efficiently shielded by the close 5 s and 5p shells. This clearly shows without doubt that the complexation of Nd(III)–DNA is effected significantly by the nature of solvents. All results obtained clearly suggest that minor coordination changes in the Nd(III) complexes are caused by coordinating sites of DNA, solvent nature, coordination number, nature of Nd(III):CT-DNA band which do induce significant variation in the intensity of 4f–4f transitions.

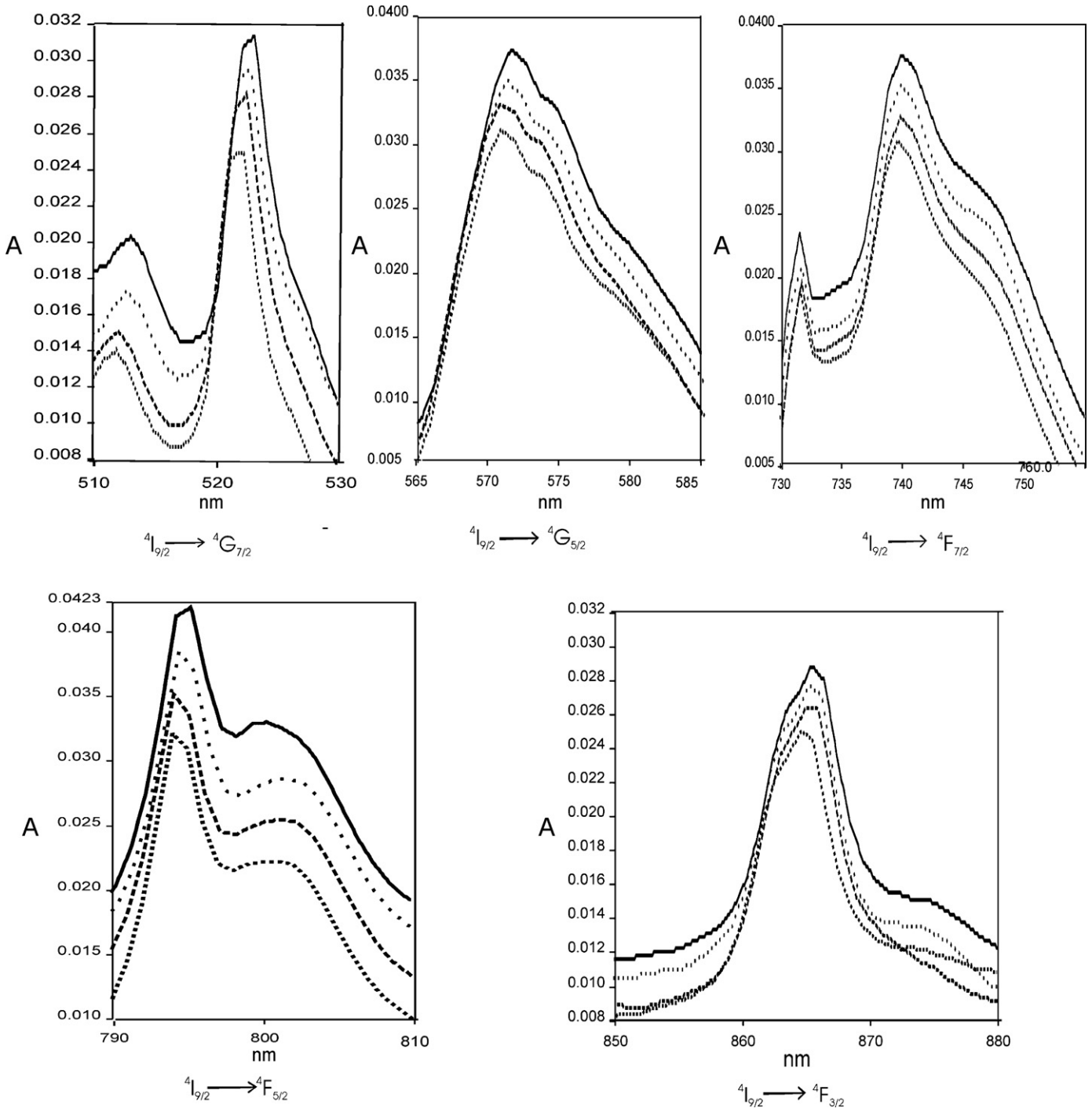

Fig. 1. Comparative absorption spectra of Nd(III)–DNA in: (A) DMF — —; (B) CH_3CN · · ·; (C) CH_3OH – – –; (D) Dioxane - - -.

3.1. Absorption titration

Absorption titration are carried out in a quartz cell by adding increasing amounts of CT DNA to a solution of Nd(III) of a fixed concentration, and recording the UV-Vis spectrum after each addition. With increase in the concentration of CT DNA, there is a substantial increase in the peak intensities of 4f–4f transition bands of Nd(III), as shown in Fig. 2. The increase in intensity (absorbance) i.e. hyperchromism is observed but no shift in wavelength. This hyperchromism can be attributed to the electrostatic interaction between the metal ion with the phosphate backbone of the DNA thereby causing the stabilization of the DNA double helix by decreasing the repulsion between the negatively charged phosphate moieties [38].

Considering the variations of absorbance of the hypersensitive transition, $^4I_{9/2} \rightarrow {}^4G_{5/2}$, the intrinsic binding constant (K_b) for the interaction of Nd(III) with CT-DNA is determined from a plot of $A_0/(A - A_0)$ versus 1/[DNA] using the following equation:

$$\frac{A_0}{A\text{–}A_0} = \frac{\varepsilon_N}{\varepsilon_{N-D} - \varepsilon_N} + \frac{\varepsilon_N}{\varepsilon_{N-D} - \varepsilon_N} \frac{1}{K_b\,[\mathrm{DNA}]} \tag{12}$$

where "A_0" and "A" are the absorbance of Nd(III) in the absence and presence of DNA, ε_N and ε_{N-D} are their absorption coefficients respectively. N and N–D represents the Calf-thymus DNA

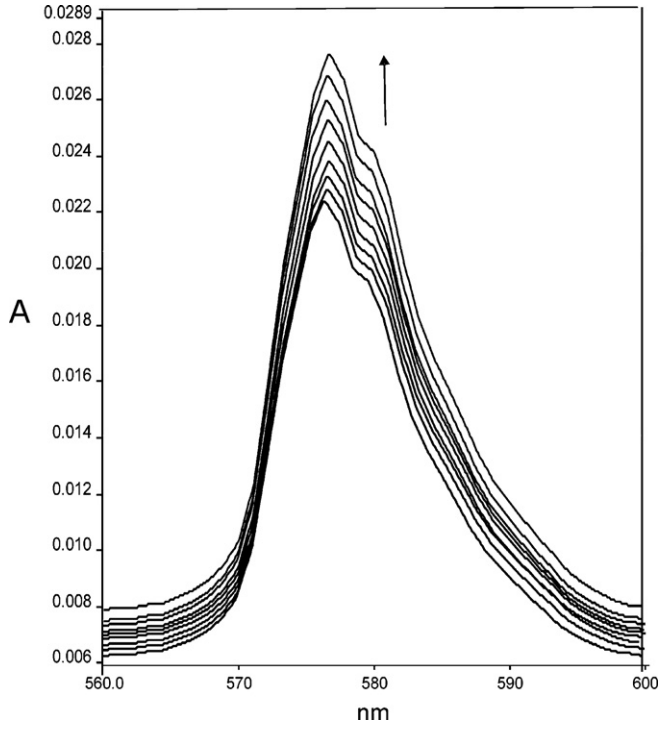

Fig. 2. Changes in the absorption bands of Nd(III), $^4I_{9/2} \rightarrow {}^4G_{52}$ upon addition of calf thymus DNA. [Nd(III)] = 20 μM and [DNA] = 0–80 μM in aqueous medium.

and Nd(III)–DNA species. The result of fitting the experimental data with Eq. (12) is shown in Fig. 3. From the plot of $A_0/(A–A_0)$ versus 1/[DNA], the ratio of intercept to the slope gives the binding constant, 9.59×10^2 L mol^{-1} at 25 °C.

3.2. Viscosity measurement

It is known that viscosity measurement is sensitive to the change in the length of the DNA double helix. In the absence of NMR and X-ray crystallographic data, viscosity measurement is considered as one of the most unambiguous methods to determine the mode of binding in solution [39]. The classical intercalation mode demands that the DNA helix lengthens as base pairs are separated to accommodate the bound ligand, leading to the increase of DNA viscosity. The value of relative specific viscosity $(\eta/\eta_0)^{1/3}$ of DNA in the presence of Nd(III) are plotted against the concentration of metal ion (Fig. 4). We see that specific viscosity of DNA decreases with increase in the concentration of Nd(III), which is not similar to that of the classical intercalation [40]. From this measurement we can suggest that the metal Nd(III) is not bound by classical interaction but bound electrostatically to the phosphate group which causes the stabilization of the DNA double helix by decreasing the repulsive forces between neighbouring negatively charged phosphate group that tend to unwind the helix thereby reducing its effective length, concomitantly. This is in agreement with our absorption experiments.

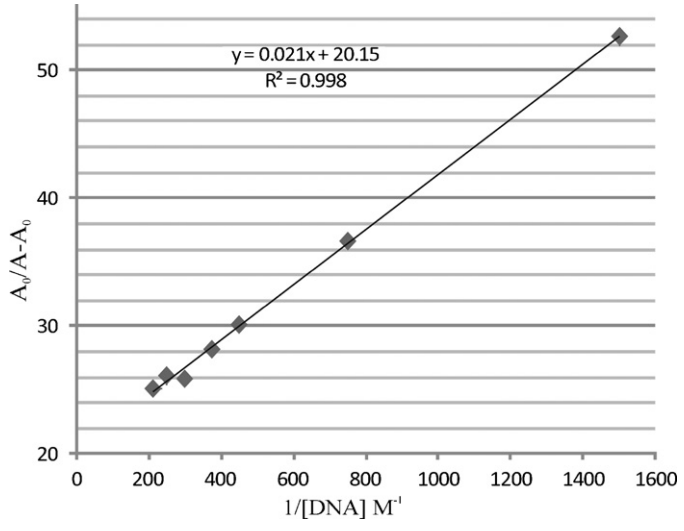

Fig. 3. The plot of $(A_0/A - A_0)$ versus (1/[DNA]). Conditions: Tris–HCl buffer (0.01 mol L^{-1}, pH 7.4), [DNA] = 2×10^{-4} mol L^{-1}.

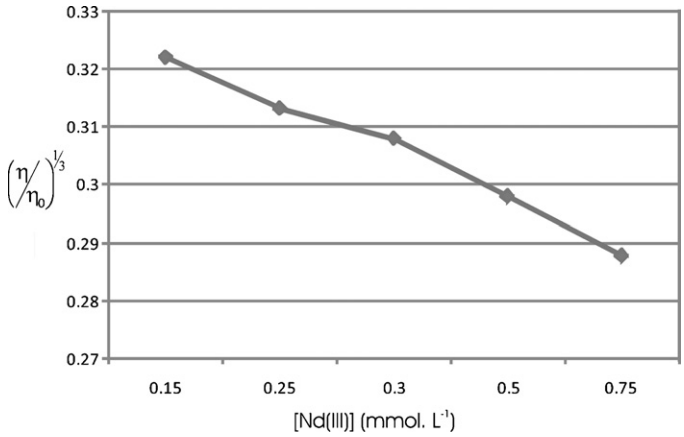

Fig. 4. Effect of increasing concentrations of metal ion on the relative viscosity of DNA in aqueous medium. [Nd(III)] = 1×10^{-4}–5×10^{-4} mol L^{-1}.

3.3. Determination of Thermodynamic parameters

Considering the dependence of binding constant on temperature, a thermodynamic process was considered to be responsible for the formation of a complex. Therefore, the thermodynamic parameters dependent on temperature were analysed in order to further characterise the interaction forces between Nd(III) and DNA. The interaction forces between a small molecule and macromolecule mainly include hydrogen bonds, van der Walls force, electrostatic force and hydrophobic interaction force. The thermodynamic parameters of binding reaction are the main evidence for confirming the binding force.

If the enthalpy change (ΔH°) does not vary significantly over the temperature range studied, then its value and that of entropy change (ΔS°) can be determined from the Van't Hoff equation:

$$\ln K = -\frac{\Delta G}{RT} = -\frac{\Delta H^\circ}{R}\left(\frac{1}{T}\right) + \frac{\Delta S^\circ}{R} \quad (13)$$

where K and R are binding constant and gas constant respectively. The binding studies were carried out at 293, 298, 303, 308, 313 and 318 K. The enthalpy change (ΔH°) and entropy change (ΔS°) were obtained from the slope and intercept of the linear Van't Hoff plot based on $\ln K$ versus $1/T$ (Fig. 5). The free energy change (ΔG°) is estimated from the following relationship:

$$\Delta G^\circ = \Delta H^\circ - T\Delta S^\circ \quad (14)$$

The values of ΔH°, ΔS° and ΔG° are listed in Table 4. The positive enthalpy and entropy values indicates that the mode of binding is an endothermic and entropy increasing process. Because $T\Delta S^\circ > \Delta H^\circ$ and the entropy increasing effect result in $\Delta G^\circ < 0$, the mode of binding is an entropy driven process. This can be explained as follows: the hydrated metal ion should lose some water molecules when they approach to the binding sites and simultaneously, the hydration layer of the DNA molecule at the

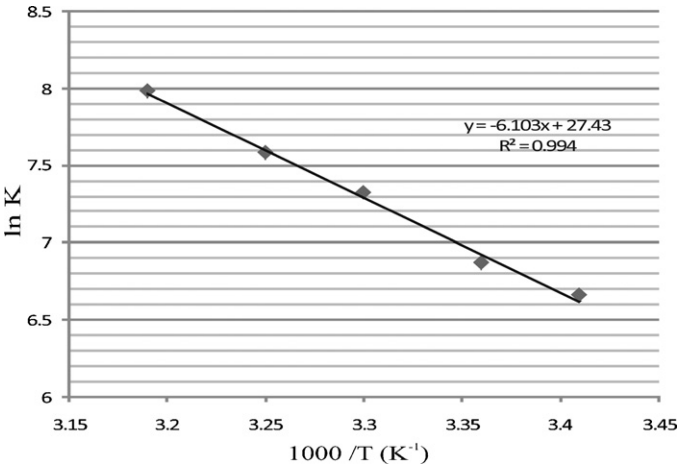

Fig. 5. Van't Hoff plot for the interaction of Nd(III) with CT-DNA in aqueous medium.

Table 4
Thermodynamic parameters of the interaction of Nd(III) with DNA in aqueous medium, at different temperatures.

T (K)	ΔH° (kJ mol^{-1})	ΔS° (J mol^{-1} K^{-1})	ΔG° (kJ mol^{-1})
293			−16.08 ± 0.01
298			−17.22 ± 0.01
303	50.74 ± 0.01	228.05 ± 0.01	−18.36 ± 0.01
308			−19.50 ± 0.01
313			−20.64 ± 0.01

binding sites should be partly destroyed. Both dehydration processes are endothermic and increase the entropy. On the other hand, small magnitude of equilibrium constant indicate that the Nd(III) only interact with phosphate moiety on the surface of the macromolecules without entering their internal cores. The interaction might include electrostatic forces and intermolecular hydrogen bonds which decrease enthalpy and entropy. The positive enthalpic and entropic changes might be overall result of the hydrogen bonds, electrostatic interaction and solvent effect [41]. Evidently in these types of binding process, the dehydration of both metal ion and DNA give rise to the positive values of enthalpic and entropic changes. Overall speaking, the negatively changes of standard Gibbs energy indicates that the mode of binding process is spontaneous processes and Nd(III)–DNA complex can form in the aqueous buffer solution.

4. Conclusions

The binding interaction of Nd(III) with DNA has been examined by absorption spectroscopy and viscosity measurements. The binding constants of Nd(III) complex with DNA were measured at different temperatures and found to be 9.59×10^2 M at 25 °C. Thermodynamic parameters indicate that the mode of binding is entropy driven process i.e. the Nd(III) ion can only interact with the phosphate group moiety on the molecular surface of the DNA.

Acknowledgements

The authors thank CSIR, New Delhi for financial support. Ch. Victory Devi, thanks CSIR, New Delhi for providing financial assistance under Senior Research Fellowship Scheme.

References

[1] L. Stryer, Biochemistry, W.H. Freeman and Company, San Francisco, CA, 1994.
[2] L.H. Hurley, Nat. Rev. Cancer 2 (2002) 188–194.
[3] H. Mansouri-Torshizi, M. Islami-Moghaddam, A. Divsalar, A.A. Saboury, Bioorg. Med. Chem. 16 (2008) 9616–9620.
[4] G.L. Eichhorn, Advances in Inorganic Biochemistry, vol. 3, Elsevier, New York, 1981, p. 2.
[5] C. Bunzli, G.R. Chopin, Lanthanide Probes in Life, Chemical and Earth Sciences: Theory and Practice, Elsevier, Amsterdam, 1989.
[6] D. Costa, H. Burrows, M. Miguel, Langmuir 21 (2005) 10492–10496.
[7] M. Tapia, H. Burrows, Langmuir 18 (2002) 1872–1876.
[8] L.G. Marzilli, Prog. Inorg. Chem. 23 (1977) 255–378.
[9] J. Reuben, in: K.A. Gschneider, L. Eyring (Eds.), Handbook on the Physics and Chemistry of Rare Earths, vol. 4, North-Holland, Amsterdam, 1979, p. 515.
[10] W.D. Horrocks Jr., D.R. Sudnick, Acc. Chem. Res. 14 (1981) 384–392.
[11] J.C.G. Bunzli, Chem. Lett. 38 (2009) 104–106.
[12] J. Hovinen, P.M. Guy, Bioconj. Chem. 20 (2009) 404–406.
[13] I. Hemmila, V. Laitala, J. Fluoresc. 15 (2005) 529–531.
[14] J. Yuan, G. Wang, TrAC Trends Anal. Chem. 25 (2006) 490–492.
[15] T. Matsuya, N. Hoshino, T. Okuyama, Curr. Anal. Chem. 2 (2006) 397–401.
[16] T. Nishioka, K. Fukui, K. Matsumoto, in: K.A. Gschneidner Jr., J.C.G. Bunzli, V.K. Pecharsky (Eds.), Handbook on the Physics and Chemistry of rare Earths, vol. 37, Elsevier Science B.V., Amsterdam, 2007.
[17] C.M. Spangler, C. Spangler, M. Schaerling, Ann. N.Y. Acad. Sci. 1130 (2008) 138–140.
[18] S.N. Misra, Indian J. Biochem. Biophys. 27 (1990) 284–288.
[19] G. Joseph, K. Anjaih, K. Venkatabramanian, H.C. Bajaj, S.N. Misra, Indian J. Chem. Sec. A 29 (1990) 346–351.
[20] C.R. Cantor, P.R. Schimmel, Biophysical Chemistry, W.H. Freeman and Co., San Francisco, CA, 1980, p. 1371.
[21] Th. David Singh, Ch. Sumitra, N. Yaiphaba, H. Debecca Devi, M. Indira, N. Rajmuhon Singh, Spectrochim. Acta A 61 (2005) 1219–1225.
[22] Th. David Singh, Ch. Sumitra, N. Rajmuhon Singh, M. Indira, J. Chem. Sci. 116 (6) (2004) 303–309.
[23] D.E. Henrie, G.R. Choppin, J. Chem. Phys. 49 (1968) 477–481.
[24] S.P. Sinha, Spectrochim. Acta 22 (1966) 57–62.
[25] K. Jorgensen, Modern Aspects of Ligand Field Theory, North-Holland, Amsterdam, 1971.
[26] K.J. Shah, M.K. Shah, Bull. Pure Appl. Sci. 20C (2001) 81–86.
[27] B.R. Judd, Opt. Phys. Rev. 127 (1962) 750–761.
[28] G.S. Ofelt, Phys. J. Chem. Phys. 37 (3) (1962) 511–520.
[29] Th. David Singh, Ch. Sumitra, G.C. Bag, M. Indira Devi, N. Rajmuhon Singh, Spectrochim. Acta A 63 (2006) 154–159.
[30] Ch. Sumitra, Th. David, M. Indira, N. Rajmuhon Singh, J. Alloys Compd. 451 (2007) 365–371.
[31] R.D. Peacock, Structure and Bonding, vol. 22, Spring-Verlag, New York/Heidelberg/Berlin, 1975, p. 104.
[32] C.K. Jorgensen, L. Ryan, J. Phys. Chem. 70 (1966) 2845–2847.
[33] S.T. Frey, W.D. Horrocks Jr., Inorg. Chim. Acta 229 (1995) 383–390.
[34] K.B. Goerller-walrand, in: K.A. Gscheidner Jr., L. Eyring (Eds.), Handbook of the Physics and Chemistry of Rare Earths, 25 vols., North-Holland, Amsterdam, 1998, p. 101 (Chapter 167).
[35] S.F. Mason, Struct. Bond. (Berl.) 39 (1980) 43–75.
[36] M.F. Reid, F.S. Richardson, J. Phys. Chem. 88 (1984) 3579–3585.
[37] W. Strek, Theor. Chim. Acta 52 (1979) 45–49.
[38] G.Y. Han, P. Yang, J. Inorg. Biochem. 91 (2002) 230–236.
[39] B. Norden, T. Tjernal, Biopolymers 21 (1981) 1713–1718.
[40] T.M. Kelly, A.B. Tossi, D.J. McConnel, C. OhUigin, Nucleic Acids Res. 17 (1985) 6017–6021.
[41] P.D. Ross, S. Subramanian, Biochemistry 20 (1981) 3096–3099.